ELSEVIER

FEBS Letters 337 (1994) 145–151

FEBS 13512

FEBS LETTERS

Elucidation of the poly-L-proline binding site in *Acanthamoeba* profilin I by NMR spectroscopy

Sharon J. Archer[a], Valda K. Vinson[b], Thomas D. Pollard[b], Dennis A. Torchia[a,*]

[a]*Bone Research Branch, Building 30, Room 106, National Institute of Dental Research, National Institutes of Health, Bethesda, MD 20892, USA*
[b]*Department of Cell Biology and Anatomy, The Johns Hopkins University School of Medicine, Baltimore, MD 21205, USA*

Received 16 November 1993; revised version received 29 November 1993

Abstract

The multifunctional protein profilin is one of the most abundant proteins in the cytoplasm and is thought to regulate actin assembly and the phosphoinositide signaling pathway. Profilin binds to several different ligands including actin, poly-L-proline, and the head groups of polyphosphoinositides. Knowledge of profilin/ligand interactions is important for understanding the physiology of profilin in the cell. As a first step in the characterization of profilin/ligand complexes, we have studied a profilin/poly-L-proline complex in solution using high resolution NMR spectroscopy. Analysis of profilin NOE's and chemical shift data indicates that the protein secondary structure is conserved upon binding to poly-L-proline and that the binding site is located between the N- and C-terminal helices in a region rich in highly conserved aromatic sidechains. This site is adjacent to the proposed binding site for actin. In addition, the rate constant for dissociation of the complex is found to be $1.6 \pm 0.2 \times 10^4$ s^{-1}.

Key words: Binding site; Protein–protein interaction; Nuclear magnetic resonance; Nuclear magnetic resonance, two-dimensional; Profilin; Polyproline; *Acanthamoeba*

1. Introduction

Profilins are found in the cytoplasm of cells in relatively high concentrations and are required for a normal actin cytoskeleton [1]. The multifunctional profilins show substantial variation in their sequence [2] and were originally characterized for their ability to bind actin monomers and regulate the polymerization of actin filaments [3]. Profilins also bind to phosphatidylinositol-4,5-biphosphate (PIP_2) [4,5], thereby inhibiting the production of the second messengers inositol trisphosphate and diacylglycerol [6,7]; this observation suggests that profilins are involved in transmembrane signaling. Furthermore, since PIP_2 inhibits the binding of profilins to actin [4,5], profilins may link transmembrane signaling and regulation of the cytoskeleton.

Profilins have the unusual ability to bind to poly-L-proline containing at least ten proline residues [8,9]. The profilin/poly-L-proline complex binds to actin or PIP_2 ([10]; and Kaiser, unpublished). The biological significance of the binding of poly-L-proline by profilin is not known [1], but it is reasonable to suppose that profilins bind to a proline-rich segment of another protein.

Because profilins function by binding to various macromolecular ligands, definition of these binding sites at atomic resolution would be of great value in understanding the mechanism of action of profilins. The three-dimensional solution structure and complete NMR signal assignments have been reported for the 13 kDa *Acanthamoeba* profilin I [11,12]. Because of its size, 55 kDa, the profilin/actin complex is a formidable challenge for NMR structural studies. The profilin/PIP_2 and profilin/PIP complexes are also too large for solution phase NMR studies because PIP and PIP_2 form micelles in solution. In contrast, the profilin/poly-L-$proline_{10}$ complex, 14 kDa, is highly amenable to NMR spectroscopy. Herein we report the profilin residues that interact with poly-L-$proline_{10}$ based upon measurements of chemical shift perturbations.

*Corresponding author. Fax: (1) (301) 402-0824.

Abbreviations: CSI, chemical shift index; CT, constant time; HMQC, heteronuclear multiple quantum correlation; TOCSY, totally correlated spectroscopy; HSQC, heteronuclear single quantum correlation; NMR, nuclear magnetic resonance; NOE, nuclear Overhauser effect; NOESY, NOE spectroscopy; PIP, phosphatidylinositol-4-phosphate; PIP_2, phosphatidylinositol-4,5-bisphosphate; 2D, two-dimensional; 3D, three-dimensional.

2. Materials and Methods

2.1. Sample preparation

Recombinant *Acanthamoeba* profilin I was uniformly enriched with ^{15}N and ^{13}C and purified as described previously [11]. Unlabeled poly-L-proline, DP = 10, was obtained by chemical synthesis (Johns Hopkins Medical School Protein-Peptide Facility). Concentrations of poly-L-

SSDI 0014-5793(93)E1429-P

proline are expressed per decamer. The concentration of ^{15}N,^{13}C-enriched profilin was ca. either 1.0 mM or 0.1 mM. For the more highly concentrated (1.0 mM) samples, the sample volumes were ca. 430 μl in 5-mm Wilmad NMR tubes (Wilmad Glass Co., Buena, NJ) or 230 μl in restricted-volume Shigemi NMR tubes (Shigemi Standard & Joint Co. Ltd., Tokyo, Japan). For the low concentration (0.1 mM) samples, the sample volumes were ca. 1.5 ml in 8-mm Wilmad NMR tubes.

The 0.1 mM profilin sample was titrated with aliquots of a concentrated solution of poly-L-proline$_{10}$ which also contained 0.1 mM profilin so that addition of poly-L-proline did not change the profilin concentration.

2.2. NMR spectroscopy

NMR spectra of profilin were acquired on a triple channel Bruker AMX 500 spectrometer. NMR spectra were processed using a combination of in-house (F. Delaglio, 'nmrPipe', unpublished) and NMRi (New Methods Research Inc., Syracuse, NY) software, and were analyzed and plotted using in-house software [13].

All spectra were acquired at 30°C. 2D ^{1}H–^{15}N HSQC [14] spectra were acquired on uniformly ^{15}N,^{13}C-labeled profilin in 93% H_2O/ 7% D_2O in the presence and absence of poly-L-proline, DP = 10. The water signal was suppressed using mild presaturation ($\gamma B_2/2\pi$ ca. 20 Hz) and a 1 ms spin-lock pulse [15]. A composite 180° carbon pulse centered at 130 ppm was applied during ^{15}N evolution to remove $^{1}J_{NC'}$ and $^{1}J_{NC\alpha}$ couplings.

2D ^{1}H–^{13}C CT-HSQC spectra of uniformly ^{15}N,^{13}C-labeled profilin in D_2O in the presence and absence of poly-L-proline were acquired as described by Vuister and Bax [16]. 2D ^{1}H–^{13}C CT-HSQC spectra in H_2O were acquired using the same pulse scheme but starting with ^{13}C magnetization while saturating proton magnetization with a series of high power pulses thus generating the heteronuclear $^{13}C\{^{1}H\}$NOE [17]. The 2D ^{1}H–^{13}C CT-HSQC spectrum was optimized for aromatic resonances by setting the inept transfer delay to 1.6 ms (slightly less than $1/4J_{CH(arom)}$) and setting the constant time carbon evolution period to 18.2 ms to refocus the carbon–carbon couplings of 55 Hz. The spectra were acquired with the ^{1}H carrier set at 4.72 ppm (water) and the ^{13}C carrier set at 126 ppm, with spectral widths of 39.8 ppm in F_1 (^{13}C) and 10.0 ppm in F_2 (^{1}H), 90 complex points in t_1, and 512 complex points in t_2. 2D ^{1}H–^{13}C CT-HSQC-RELAY spectra were recorded using the same HSQC experiments with a 22 ms ^{1}H WALTZ-17 mixing sequence inserted between the last refocusing period and data acquisition. In all heteronuclear experiments, GARP and WALTZ-16 modulations [18] were used during acquisition to decouple ^{13}C and ^{15}N, respectively.

A 3D ^{15}N separated NOESY-HMQC [19, 20] experiment was acquired on 0.8 mM ^{15}N,^{13}C-labeled profilin with 16.7 mM poly-L-proline in 93%H_2O/7%D_2O. The spectrum was acquired with a 110 ms mixing time and ^{13}C decoupling was accomplished with a composite 180° ^{13}C pulse centered at 46 ppm during ^{1}H evolution (t_1) and a 180° ^{13}C pulse centered at 130 ppm during ^{15}N evolution (t_2). The ^{1}H carrier was set at 4.72 ppm (water) and the ^{15}N carrier at 118.0 ppm. The spectrum was acquired with spectral widths of 10.00, 22.9 and 11.76 ppm in F_1 (^{1}H), F_2 (^{15}N) and F_3 (^{1}H), respectively, 128 complex points in t_1, 32 complex points in t_2, 512 complex points in t_3, and 16 scans per fid.

3D triple resonance CBCA(CO)NH [21] and CBCANH [22] experiments were acquired on 0.8 mM ^{15}N,^{13}C-labeled profilin with 16.7 mM poly-L-proline in 93%H_2O/7%D_2O. These spectra were acquired with spectral widths of 67.16, 29.9 and 15.15 ppm in F_1 (^{13}C), F_2 (^{15}N) and F_3 (^{1}H), respectively, and with 52 complex points in t_1, 32 complex points in t_2, 512 complex points in t_3 and 16 scans per fid for the CBCA(CO)NH and 32 scans per fid for the CBCANH. The carrier was set at 46 ppm for $C_{\alpha/\beta}$ pulses and at 56 ppm for C_α pulses and the pulse lengths were adjusted so that they did not excite the ^{13}CO nuclei. The ^{1}H carrier was set on water and the ^{15}N carrier was set at 118.0 ppm.

3. Results

The chemical shifts and linewidths of all amide resonances of ^{15}N, ^{13}C-labeled profilin (114 backbone and 26 sidechain amide peaks) were monitored as a function of poly-L-proline concentration in the ^{1}H–^{15}N HSQC spectra (Fig. 1A). The addition of poly-L-proline shifts the positions of many amide cross-peaks (Fig. 1B). Although the linewidths of most signals increase slightly (0.2–0.3 Hz) with the addition of poly-L-proline, the linewidths of those signals that show the largest change in their chemical shifts increase by 1–8 Hz (Table 1). Because these increases in linewidth, ΔW, are small compared with the chemical shift differences, $\Delta\upsilon = \upsilon_a - \upsilon_b$, in the free, *a*, and bound, *b*, states (Table 1), one can calculate the dissociation rate constant of the profilin–poly-L-proline complex, k_b. Recasting the fast exchange form of the Gutowsky-Holm equation [23,24] to calculate the lifetime of the bound state τ_b (= $1/k_b$) renders:

$$\tau_b = \Delta W/4\pi(1 - p_b)^2 p_b \Delta\upsilon^2 \quad (1)$$

where p_b, the relative population of the bound profilin, is equal to $(\upsilon - \upsilon_a)/\Delta\upsilon$. Values of τ_b calculated for residues having the largest (and hence most accurate) values of ΔW are listed in Table 1 for $p_b = 0.3$. From the results tabulated in Table 1, we find $<\tau_b> = 6.3 \pm 0.7 \cdot 10^{-5}$ s and $<k_b> = 1/<\tau_b> = 1.6 \pm 0.2 \cdot 10^4$ s^{-1}. The weighted average was obtained from $<\tau_b> = \Sigma(\tau_i/\varepsilon_i^2)/\Sigma(1/\varepsilon_i^2)$ where

Table 1
Values of τ_b calculated at $p_b = 0.3$[a] using Eq. 1 together with the listed values of $\Delta\upsilon$ and ΔW[b]

Residue	Atom	$\Delta\upsilon$ (Hz)	ΔW (Hz)	$\tau_b \times 10^4$ (s)
W2	Hε1	265	7.8 ± 1.0	0.60 ± 0.08
T4	HN	80	1.9 ± 1.0	1.6 ± 0.8
L120	HN	115	3.2 ± 1.0	1.3 ± 0.4
Q123	Nε	74	1.2 ± 0.6	1.2 ± 0.6
Q123	Hε1	100	2.5 ± 1.0	1.4 ± 0.5
Q123	Hε2	125	3.8 ± 1.0	1.3 ± 0.4
F125	HN	195	2.9 ± 1.0	0.4 ± 0.1

[a] Data obtained at $p_b = 0.3$ were used to calculate τ_b since equation 1 shows that ΔW is largest at $p_b = 1/3$.

[b] The listed value of ΔW is 0.2 Hz (^{15}N) or 0.3 Hz (^{1}H) less than measured in order to correct for the increase in line-width observed for residues having $\Delta\upsilon = 0$ which we ascribe to the increased molecular weight of the complex as compared with free profilin.

→

Fig. 1. (A) ^{1}H–^{15}N HSQC spectrum of the complex of profilin with poly-L-proline$_{10}$ at 30°C and pH 6.4. The sample contained approximately 0.8 mM ^{15}N,^{13}C-labeled profilin and 16.7 mM poly-L-proline$_{10}$ in 93% H_2O/7% D_2O. The peak positions in this spectrum were compared with the peak positions in an HSQC spectrum acquired on 1.2 mM profilin free in solution. The labeled cross-peaks correspond to residues whose amide ^{1}H or ^{15}N chemical shifts change significantly (> 0.05 ppm in ^{1}H chemical shift or > 0.25 ppm in ^{15}N chemical shift) in the presence of poly-L-proline$_{10}$. (B) Plots of chemical shift differences, $\Delta\delta$, versus residue number for the amide ^{1}H and ^{15}N resonances for profilin in the absence and presence of poly-L-proline. Chemical shift values were determined from ^{1}H–^{15}N HSQC experiments.

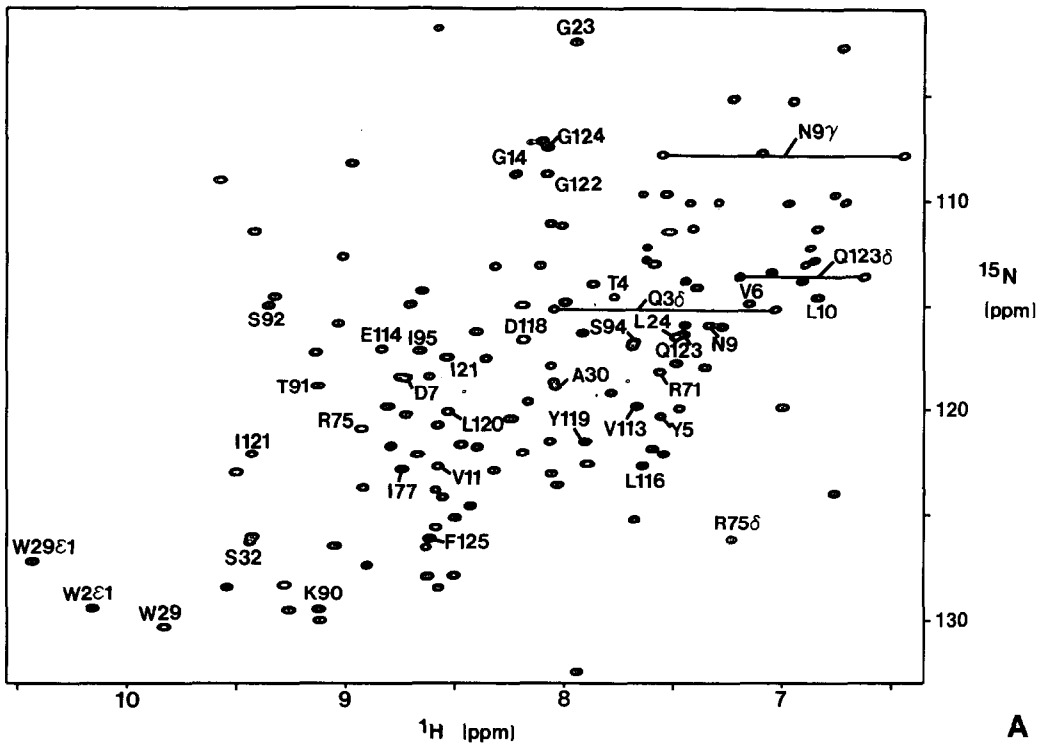
G23
G124
G14
G122
N9γ
Q123δ
T4
Q3δ
V6
L10
S92
E114
I95
D118
S94
L24
Q123
N9
I21
A30
R71
T91
D7
R75
L120
Y119
V113
Y5
I121
V11
L116
I77
R75δ
W29ε1
F125
S32
W2ε1
K90
W29
10
9
8
7
110
120
130
15N (ppm)
1H (ppm)
A

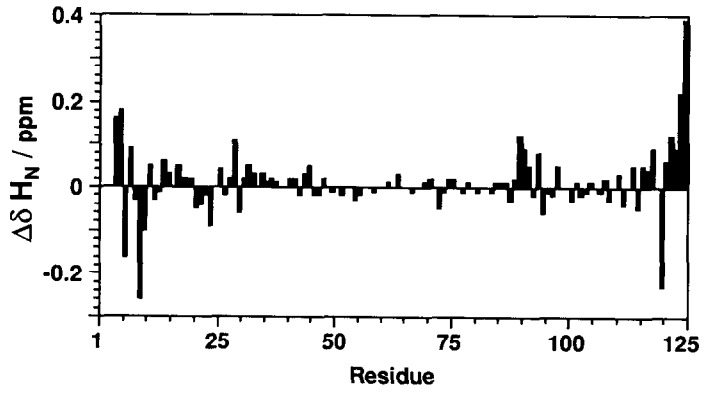
0.4
0.2
0
-0.2
ΔδHN / ppm
1
25
50
75
100
125
Residue

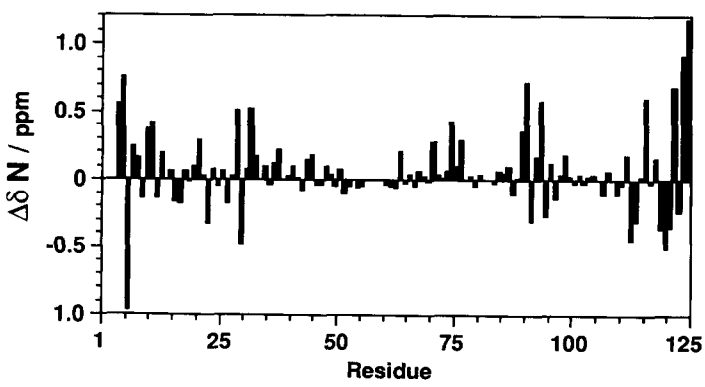
1.0
0.5
0
-0.5
1.0
ΔδN / ppm
1
25
50
75
100
125
Residue
B

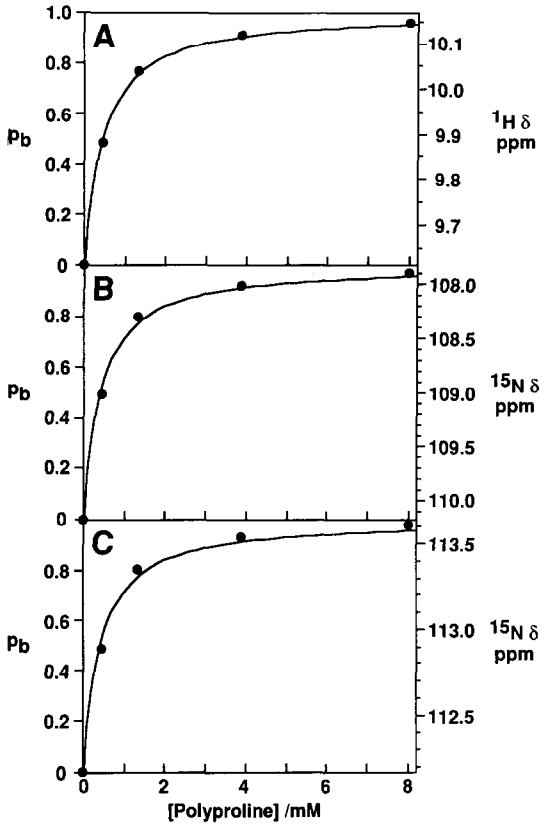

Fig. 2. Titration of 0.1 mM profilin with poly-L-proline$_{10}$. The chemical shift (right axis) and the calculated fraction bound, p_b, (left axis) of (A) Hε1 of W2, (B) Nδ of N9 and (C) Nε of Q123 are plotted (solid points) as a function of poly-L-proline concentration. The solid line is a theoretical binding curve calculated assuming a fast exchange 1:1 complex with (A) K_d = 410 μM, (B) K_d = 370 μM and (C) K_d = 370 μM.

the summation extended over the τ_b values listed in Table 1 and ε_i is the error in the i-th τ_b value.

Profilin was titrated with poly-L-proline at both a high (1 mM) and a low (0.1 mM) profilin concentration. The chemical shifts of all amide resonances in the ^{1}H–^{15}N HSQC spectrum of 0.1 mM profilin are identical to those in the spectrum of 1.0 mM profilin, under conditions where nearly all of the profilin (ca. 95%) is bound to poly-L-proline, namely, 0.8 mM profilin plus 16.7 mM poly-L-proline and 0.1 mM profilin plus 8.0 mM poly-L-proline.

The chemical shift differences of amide resonances that shifted significantly with added poly-L-proline were plotted as a function of poly-L-proline concentration to determine the binding constant (Fig. 2). At the lower profilin concentration, 0.1 mM, best fits of the data were obtained for K_d values ranging from 0.37 to 0.41 mM. Scatchard analysis of the data assuming a protein:ligand ratio of 1:1 produced linear Scatchard plots which were also used to calculate the dissociation constant K_d. Dissociation constants K_d calculated from Scatchard analysis range from 0.42 to 0.46 mM. A dissociation equilibrium constant of 0.4 mM together with the value of k_b determined from the excess linewidths yields an association rate of 4×10^7 s$^{-1} \cdot$ M^{-1} ($k_b/0.4 \times 10^{-3}$ M).

In contrast to the results obtained at the low profilin concentration, titrations done at 1.0 mM profilin did not exhibit a simple binding behavior, and the data were not well fit by a simple one-site binding curve. An apparent dissociation constant equal to ca. 1.2 mM gave the best fitting curve. Although the binding curves observed for high concentrations of profilin are non-ideal, it was found that, for a given value of p_b, the ^{1}H–^{15}N HSQC spectrum of the profilin–poly-L-proline complex at 1 mM profilin was the same as the spectrum obtained at 0.1 mM profilin. This observation implies that the conformation of profilin in the profilin–polyproline complex observed at 1 mM is the same conformation observed at 0.1 mM.

Changes in profilin ^{1}H and ^{15}N chemical shifts that accompany poly-L-proline binding vary in magnitude along the polypeptide chain (Fig. 1B). Backbone amides that exhibit substantial chemical shift changes ($|\Delta\delta$H$| > 0.10$ ppm or $|\Delta\delta$N$| > 0.5$ ppm) are T4, Y5, V6, N9, W29, S32, K90, T91, S94, L116, L120, G122, G124, and F125. The sidechain amides of W2, N9, W29 and Q123 also undergo substantial chemical shift changes in the presence of poly-L-proline, namely, W2, $\Delta\delta$H = 0.53 ppm; N9, $\Delta\delta$N = −2.3 ppm; W29, $\Delta\delta$N = −0.7 ppm; Q123, $\Delta\delta$N = −1.5 ppm. Backbone amides that exhibit modest chemical shift changes ($0.05 < |\Delta\delta$H$| < 0.10$ ppm or $0.25 < |\Delta\delta$N$| < 0.5$ ppm) include D7, L10, V11, G14, I21, G23, L24, A30, R71, R75, I77, S92, I95, V113, E114, D118, Y119, I121, Q123. The sidechain amides of Q3 and R75 also exhibit modest chemical shift changes, namely, $\Delta\delta$H = −0.07 ppm for Q3 and $\Delta\delta$N = −0.27 ppm for R75.

A 2D ^{1}H–^{13}C CT-HSQC experiment optimized for aromatic resonances was acquired on 0.8 mM profilin in the presence of 16.7 mM poly-L-proline and compared with a spectrum acquired on free profilin. A 2D CT-HSQC-RELAY was acquired on profilin/poly-L-proline to confirm the assignments of the aromatic resonances that shifted due to the presence of poly-L-proline. Residues W2, Y5, W29 and Y119 have at least one sidechain atom that exhibits a significant chemical shift change ($|\Delta\delta$H$| > 0.10$ ppm or $|\Delta\delta$C$| > 0.4$ ppm). The cross peaks corresponding to F125 could not be identified in the CT-HSQC or the CT-HSQC-RELAY. The Cε1 proton of H66 exhibited a small chemical shift change ($\Delta\delta$H = 0.07 ppm) between the sample of profilin in D_2O and the sample of profilin with 20 mM poly-L-proline in H_2O.

A 3D ^{15}N separated NOESY-HMQC acquired on 0.8 mM ^{15}N,^{13}C-labeled profilin in the presence of 16.7 mM poly-L-proline was compared with a 3D NOESY-HMQC acquired on 1.2 mM ^{15}N-labeled profilin using similar acquisition parameters. Overall, the intensities of the NOE cross-peaks are weaker for profilin in the

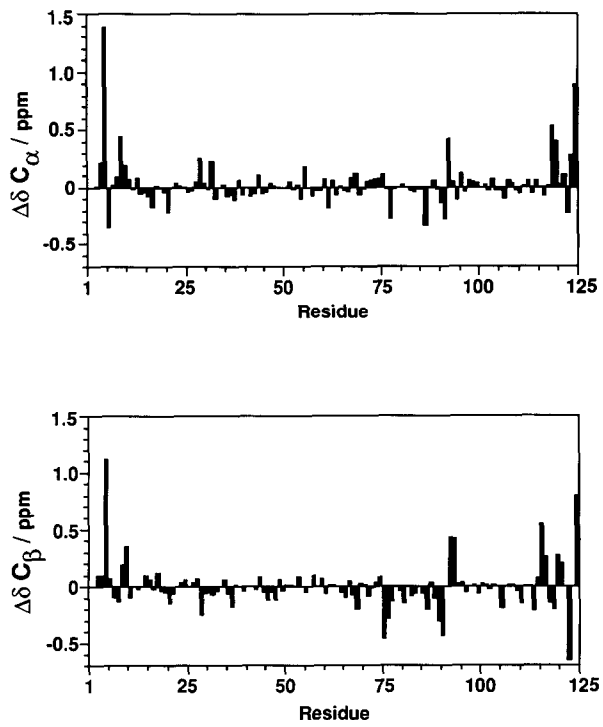

Fig. 3. Plots of chemical shift differences, $\Delta\delta$, versus residue number for the $^{13}C_\alpha$ and $^{13}C_\beta$ resonances for profilin in the absence and presence of poly-L-proline. Chemical shift values were determined from CBCA(CO)NH and CBCANH experiments.

presence of poly-L-proline due to the lower sample concentration and the shorter ^1H T_2 relaxation times for protons directly attached to ^{13}C-labeled carbons. A systematic comparison of the relative intensities of the amide-amide and amide-aliphatic proton NOE cross-peaks amides indicates that the conformation of the protein backbone has not changed significantly in the presence of poly-L-proline. Even backbone amide protons that show large changes in chemical shift still retain the same relative NOE cross-peak intensities.

The chemical shifts of the C_α and C_β carbons in the CBCANH and CBCA(CO)NH experiments acquired in the presence of poly-L-proline were compared with the C_α and C_β shifts for profilin alone (Fig. 3). Many residues exhibited greater than 0.2 ppm difference in either the C_α or C_β chemical shift: T4, Y5, V6, N9, L10, I21, W29, S32, S76, I77, Y78, I87, K90, T91, S92, K93, S94, E114, L116, A117, Y119, L120, I121, Q123, G124, F125. These residues cluster in the same regions of the protein where we see changes in the backbone HN and N chemical shifts.

C_α and C_β chemical shifts are reliable indicators of regular secondary structure elements in proteins [25,26]. Following the Chemical Shift Index (CSI) [26], we used C_α chemical shifts to identify elements of secondary structure for profilin and profilin complexed with poly-L-proline (Fig. 4). Elements of secondary structure in profilin determined using the CSI agree well with elements of secondary structure determined from NOE data. A few minor differences between the CSI prediction and the NOE derived secondary structure were observed. The CSI identifies all three helices, six of seven β-strands and one additional β-strand. The additional β-strand spans residues 35–38 and is consistent with the ϕ,ϑ angles for these residues determined from NOE and coupling constant data. The CSI predicts slightly longer N- and C-terminal helices than the NOE data and misses the short second β-strand (A30–A33). Although this short sheet has two residues with upfield shifted C_α resonances, three upfield shifted resonances are needed to strictly classify it as β-strand using the CSI. The CSI predicts that the secondary structure of profilin is virtually unchanged when the protein binds to poly-L-proline. Only two minor differences are indicated: (1) the first CSI β-strand now ends at the same residue (L22) as the NOE data indicates, and (2) the last β-strand shows a break at residue G98 because of a minor change in the C_α chemical shift, 0.05 ppm, upon binding poly-L-proline. Overall, although many C_α chemical shifts change significantly with added poly-L-proline, the elements of secondary structure as determined by the CSI do not change significantly in the presence of poly-L-proline.

4. Discussion

Chemical shift perturbations are sensitive monitors of

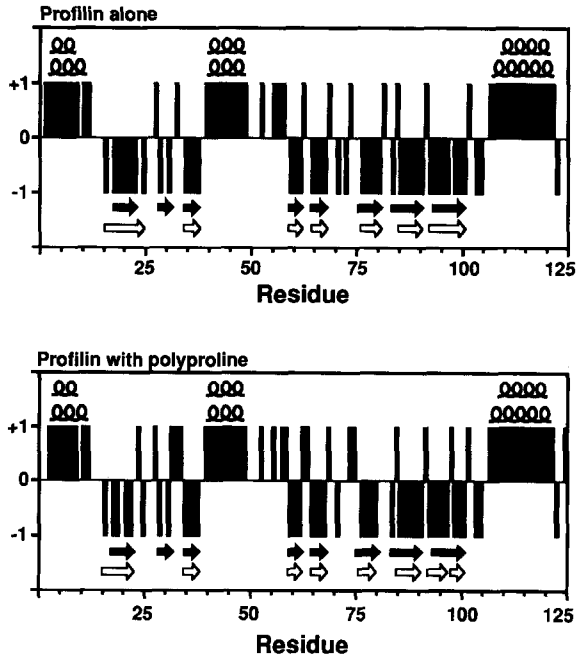

Fig. 4. Comparison of secondary structural elements obtained from NOE data (top row) and from Chemical Shift Index analysis of the C_α chemical shifts (second row) for (A) profilin and (B) profilin complexed with polyproline$_{10}$. Arrows represent β-strands as determined from NOE data for profilin (solid arrows) and from the CSI method (open arrows). Coils represent helical structures as determined from NOE data for profilin (top row) and from the CSI method (second row).

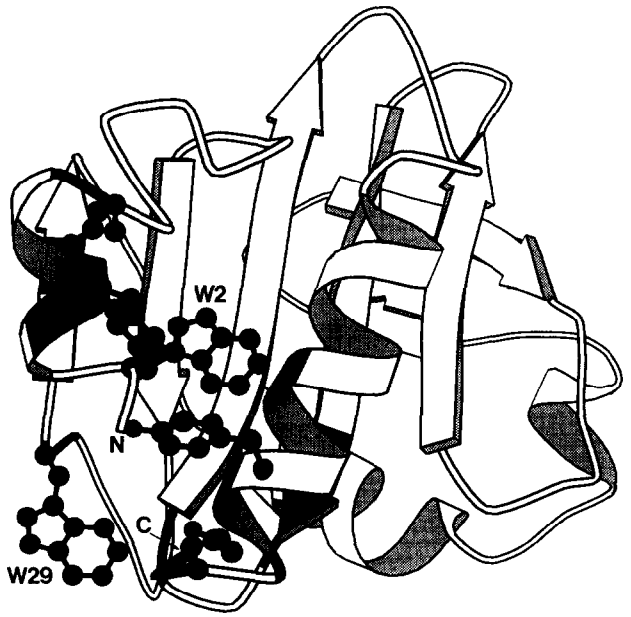

Fig. 5. Residues that show chemical shift differences in the presence of polyproline are mapped onto the three dimensional structure of *Acanthamoeba* profilin I drawn using Molscript software [38]. Residues with aromatic sidechain or backbone ^{1}H or ^{15}N resonances that exhibit substantial chemical shift changes ($|\Delta\delta H| > 0.10$ ppm or $|\Delta\delta N| > 0.5$ ppm or $|\Delta\delta C| > 0.4$ ppm) are shaded black. The sidechains are displayed only for those aromatic residues whose sidechain resonances exhibit significant chemical shift differences. The two trp sidechains and the N- and C-termini are indicated.

changes in local environments of nuclear spins and have been used to locate binding sites in several proteins [27–29]. It is gratifying that profilin residues that show large chemical shift changes, regions shaded in black in Fig. 5, map onto one continuous region of the profilin structure, as one would expect if these residues define the polyproline binding site.

Most of the residues that showed more modest, yet measurable chemical shift changes are located in the same region of the protein that show the large chemical shift changes. Some of the residues exhibiting small chemical shift perturbations are, however, not part of the poly-L-proline binding site. Other studies of chemical shift perturbations in the presence of ligands have noted that resonances that are in amino acid residues that are close to but not part of the binding site can also exhibit changes in chemical shift [29,30]. This is presumably due to the exquisite sensitivity of chemical shifts to local environments [31].

The aromatic sidechains of residues W2, W29, Y5 and Y119 show substantial changes in chemical shift in the presence of poly-L-proline. These residues are highly conserved across the profilin phylogenetic tree; W2 is conserved in all six phyla while W29 and Y5 are conserved in five of six phyla and Y119 is conserved in four of six phyla [2]. In vertebrate profilin, the conservative aromatic substitution Y119:H is present while the remaining three aromatic residues are conserved. Aromatic residues W29, Y5 and Y119 are, however, not conserved in *vaccinia* profilin where the aromatic-to-hydrophobic substitutions W29:L, Y5:I and Y119:V are found. It is noteworthy that *vaccinia* profilin, unlike the other profilins, does not bind poly-L-proline [1]. Recent mutagenesis studies of vertebrate profilin have shown that mutations of W2 and Y119 (W3 and H119 in vertebrate profilin) to asparagine and serine, respectively, abolishes poly-L-proline binding [32]. The importance of the observation that profilins that bind poly-L-proline have highly conserved aromatic residues at the poly-L-proline binding site suggests that these aromatic sidechains are essential for profilin binding to poly-L-proline.

Like profilin, the SH3 (src homology-3) domains of tyrosine kinases also bind proline rich peptides [28,33,34]. The SH3 domains are found in a wide variety of proteins, including the tyrosine kinases and actin binding proteins. The presence of SH3 domains in cytoskeletal proteins and evidence linking mutations to cellular transformation and altered morphology have led to the suggestion that the SH3 domains are involved in regulation of the cytoskeleton [28,34]. NMR studies of the association of the tyrosine kinase Src SH3 domain in the presence of proline-rich peptides derived from regions of the 3BP-1 binding protein have shown that the peptide binds to a hydrophobic surface covered with conserved aromatic amino acids [27]. Similar studies on the binding of p85α SH3 domain to a proline-rich peptide from the microtubule binding GTPase called dynamin have also shown that the peptide binding site involves aromatic amino acids that are conserved in other SH3 domains [28]. Although there are differences in the folding topology of profilin and SH3 domains [12,27,35], both proteins have several conserved aromatic sidechains lining the binding site for proline-rich peptides. Perhaps the profilin and SH3 domains regulate the cytoskeleton through interactions involving their proline binding sites.

It is also interesting to note that nine of the seventeen residues highly conserved across the profilin phylogenetic tree show perturbations in chemical shift in the presence of poly-L-proline; these residues are W2, Y5, D7, L10, I21, W29, A30, T91, and L120. The last 30 amino acids in profilin are homologous with segments in the actin binding proteins gelsolin, severin and fragmin. Only three amino acids that are highly conserved among the profilins, namely, G107, A117 and L120, are located in the region of the protein sequence that shows homology with actin binding proteins outside the profilin family, and only one of them, L120, shows chemical shift changes upon poly-L-proline binding. Hence it appears a large number of the conserved amino acids in profilins are implicated in binding to poly-L-proline rather than to actin.

The binding of polyproline to profilin has also been examined using the change in fluorescence of tryptophan residues [9]. Titration of profilin with polyproline results in an increase in fluorescence emission at 333 nm indicating that at least one of the tryptophan residues in profilin is located at the polyproline binding site. From the NMR data, both tryptophans show chemical shift perturbations in the presence of polyproline suggesting that the increase in fluorescence with added polyproline is due to both tryptophans. The binding curves determined from NMR data at 0.1 mM indicate that the dissociation constant for the profilin–polyproline complex is ca. 400 μM. A fluorescence titration curve acquired under NMR sample conditions yields a dissociation constant of ca. 100 μM. At present we cannot explain why the dissociation constants determined by these two techniques under the same conditions of pH, temperature and profilin concentration, 0.1 mM, differ by a factor of four. The fluorescence data do exhibit a considerable amount of scatter, possibly due to light scattering, that may be the source of the discrepancy.

Previous experimental evidence had shown that the actin binding site in profilin involves the C-terminal helix ([12] and references therein). More recently, the crystal structure of a gelsolin segment 1:actin complex was published which indicated that the gelsolin helix with homology to the C-terminal helix of profilin bound in a cleft on the actin surface [36]. Most recently, the crystal structure of a vertebrate profilin-actin complex was published which showed that the N-terminal portion of the C-terminal helix as well as residues from strands 4, 5, and 6, and from the helix spanning residues 57–61 (residues 54–58 in *Acanthamoeba* profilin) were involved in actin binding [37]. Using this information to define the actin binding site, the polyproline binding site identified by NMR data lies adjacent to the actin binding site. This conclusion is consistent with previous reports that profilin can bind poly-L-proline and actin simultaneously [10].

Acknowledgements: We gratefully acknowledge Dr. L. Machesky for providing fluorescence binding data. We acknowledge Drs. A. Bax, D. Garrett, S. Grzesiek, and F. Delaglio for providing pulse sequences and computer software. We also thank R. Tschudin for expert technical support. This work was supported by the AIDS Targeted Antiviral Program of the Office of the Director of the National Institutes of Health (to D.A.T.), Public Health Service National Research Service Award GM13620 (to S.J.A.), and NIH Research Grant GM-35171 (to E.E.Lattman and T.D.P.)

References

[1] Machesky, L.M. and Pollard, T.D. (1993) Trends Cell Biol. 3, 381–385.
[2] Pollard, T.D. and Rimm, D.L. (1991) Cell Motil. Cytoskel. 20, 169–177.
[3] Carlsson, L., Nystrom, L., Sundkvist, I., Markey, F. and Lindberg, U. (1977) J. Mol. Biol. 115, 465–483.
[4] Lassing, I. and Lindberg, U. (1985) Nature 314, 472–474.
[5] Lassing, I. and Lindberg, U. (1988) J. Cell. Biochem. 37, 255.
[6] Goldschmidt-Clermont, P., Kim, J., Machesky, L., Rhee, S. and Pollard, T. (1991) Science 251, 1231–1233.
[7] Machesky, L.M., Goldschmidt-Clermont, P.J. and Pollard, T.D. (1990) Cell Regul. 1, 937–950.
[8] Tanaka, M. and Shibata, H. (1985) Eur. J. Biochem. 151, 291–297.
[9] Machesky, L.M. (1993) Ph.D. Thesis, Johns Hopkins University.
[10] Kaiser, D.A., Goldschmidt-Clermont, P.J., Levine, B.A. and Pollard, T.D. (1989) Cell Motil. Cytoskel. 14, 251–262.
[11] Archer, S.J., Vinson, V.K., Pollard, T.D. and Torchia, D.A. (1993) Biochemistry 32, 6680–6687.
[12] Vinson, V.K., Archer, S.J., Lattman, E.E., Pollard, T.D. and Torchia, D.A. (1993) J. Cell Biol. 122, 1277–1283.
[13] Garrett, D.S., Powers, R., Gronenborn, A.M. and Clore, G.M. (1991) J. Magn. Reson. 95, 214–220.
[14] Bodenhausen, G. and Ruben, D.J. (1980) Chem. Phys. Lett. 69, 185–189.
[15] Messerle, B.A., Wider, G., Otting, G., Weber, C. and Wuthrich, K. (1989) J. Magn. Reson. 85, 608–613.
[16] Vuister, G.W. and Bax, A. (1992) J. Magn. Res. 98, 428–435.
[17] Kay, L.E., Torchia, D.A. and Bax, A. (1989) Biochemistry 28, 8972–8979.
[18] Shaka, A.J., Keeler, J. and Freeman, R. (1983) J. Magn. Reson. 53,
[19] Marion, D., Kay, L.E., Sparks, S.W., Torchia, D.A. and Bax, A. (1989) J. Am. Chem. Soc. 111, 1515–1517.
[20] Kay, L., Marion, D. and Bax, A. (1989) J. Magn. Reson. 84, 72–84.
[21] Grzesiek, S. and Bax, A. (1992) J. Am. Chem. Soc. 114, 6291–6293.
[22] Grzesiek, S. and Bax, A. (1992) J. Magn. Reson. 99, 201–207.
[23] Gutowsky, H.S. and Holm, C.H. (1956) J. Chem. Phys. 25, 1228.
[24] Bovey, F.A. (1969) Nuclear Magnetic Resonance Spectroscopy, Academic Press, New York.
[25] Spera, S. and Bax, A. (1991) J. Am. Chem. Soc. 113, 5490–5492.
[26] Wishart, D.S. and Sykes, B.D. (1993) J. Biomol. NMR (in press).
[27] Yu, H., Rosen, M.K., Shin, T.B., Seidel-Dugan, C., Brugge, J.S. and Schreiber, S.L. (1992) Science 258, 1665–1668.
[28] Booker, G.W., Gout, I., Downing, A.K., Driscoll, P.C., Boyd, J., Waterfield, M.D. and Campbell, I.D. (1993) Cell 73, 813–822.
[29] Chen, Y., Reizer, J., Milton H Saier, J., Fairbrother, W.J. and Wright, P.E. (1993) Biochemistry 32, 32–37.
[30] Spitzfaden, C., Weber, H.-P., Braun, W., Kallen, J., Wider, G., Widmer, H., Walkinshaw, M.D. and Wüthrich, K. (1992) FEBS Lett. 300, 291–300.
[31] Dios, A.C. d., Pearson, J.G. and Oldfield, E. (1993) Science 260, 1491–1496.
[32] Björkegren, C., Rozycki, M., Schutt, C.E., Lindberg, U. and Karlsson, R. (1993) FEBS Lett. 333, 123–126.
[33] Cicchetti, P., Mayer, B.J., Thiel, G. and Baltimore, D. (1992) Science 257, 803–806.
[34] Ren, R., Mayer, B.J., Cicchetti, P. and Baltimore, D. (1993) Science 259, 1157–1161.
[35] Musacchio, A., Noble, M., Pauptit, R., Wierenga, R. and Saraste, M. (1992) Nature 359, 851–855.
[36] McLaughlin, P.J., Gooch, J.T., Mannherz, H. and Weeds, A.G. (1993) Nature 364, 685–692.
[37] Schutt, C.E., Myslik, J.C., Rozycki, M.D., Goonesekere, N.C. W. and Lindberg, U. (1993) Nature 365, 810–816.
[38] Kraulis, P. (1991) J. Appl. Crystallogr. 24, 946–950.